Beitr. Phys. Atmosph., November 1994, p. 287–301
0005-8173/94/04 0287–15 $ 3.00/0

Remotely Sensed Water Vapor Variations during CLEOPATRA '92

by P. F. MEISCHNER[1]*, C. KIEMLE[1], G. EHRET[1], M. KÄSTNER[1], H. G. SCHREIBER[1], A. V. EVTUSHENKO[2], B. G. KUTUZA[2], B. Z. PETRENKO[2] and M. T. SMIRNOV[2]

[1]Institut für Physik der Atmosphäre, DLR Oberpfaffenhofen, 82230 Weßling, Germany
[2]Institute of Radioengineering and Electronics, RAS, Mokhovaja st. 11, Moscow 103907, Russia

(Manuscript received April 26, 1994; accepted September 29, 1994)

Abstract

Total atmospheric water vapor contents have been measured during CLEOPATRA '92 using different methods. A multifrequency microwave radiometer system from IRE, Moskow operated from ground and an airborne DIAL system, DLR, performed measurements above the radiometer site. The results compare well if the atmospheric conditions are sufficiently homogeneous in the mesoscale and complement in a high space resolution for the DIAL measurements and a high time resolution of the microwave system. Under these conditions both measurement results further agree with radiosoundings and aircraft in situ measurements within the estimated measurement errors. Coordinated observations by the different systems with high time and high space resolution open a good chance to separate between transports caused by advection or convection. Microwave radiometer measurements from ground are best suited for monitoring long term trends as well as fast fluctuations, whereas the DIAL measurements give more detailed insight in the diffusion processes within the atmospheric boundary layer ABL. The measurements on May 29 very impressively show the moisture fluxes from local lakes into the ABL. The obervations support the ABL to act as a flux-averaging medium, thus contributing naturally to an upscaling which improves the use of remote measurements from space for the estimation of area averaged moisture fluxes.

Zusammenfassung

Fernerkundung des Wasserdampfgehaltes während CLEOPATRA '92

Der Gesamtsäulenwassergehalt der Atmosphäre wurde während CLEOPATRA '92 aus verschiedenen Meßmethoden bestimmt. Ein Mehrfrequenz-Mikrowellenradiometersystem des IRE, Moskau hat vom Boden aus gemessen, während mit einem flugzeuggetragenen DIAL System der DLR über dem Mikrowellensystem nach unten gemessen wurde. Die Meßergebnisse sind gut vergleichbar bei mesoskalig homogenen Bedingungen und ergänzen sich gut, was die hohe zeitliche Auflösung der Radiometer und die hohe räumliche Auflösung des DIALs betrifft. Auch mit den Ergebnissen von Radiosondenmessungen und den Flugzeug in situ Messungen wurden im Rahmen der Meßgenauigkeiten für diese Bedingungen gute Übereinstimmungen festgestellt. Die kombinierten Messungen mit hoher zeitlicher bzw. hoher räumlicher Auflösung ermöglichen die Trennung von Feuchtetransporten durch Advektion bzw. Konvektion. Die Mikrowellen-Radiometermessungen vom Boden aus eignen sich gut zum Monitoring langzeitiger Trends und zur Beobachtung kurzzeitiger Fluktuationen, während DIAL Messungen detaillierte Einblicke in die Prozeßabläufe innerhalb der Grenzschicht vermitteln. Das Meßbeispiel vom 29. Mai zeigt sehr eindrucksvoll einen morgendlichen Feuchtefluß des Ammer- und Starnberger Sees in die trockene Grenzschicht. Die Beobachtungen in der Grenzschicht zeigen, daß diese als ein natürliches Medium der Mittelung fungiert, das oberflächenbedingte kleinräumige Feuchtefluktuationen in großräumige Strukturen überführt, wie sie dann auch z.B. von Satellitenmessungen aufgelöst werden können.

1 Introduction

The knowledge of water vapor and its variability on all atmospheric scales is of fundamental importance for a better understanding of the meteorological, hydrological and climatological processes and their interactions. The energy exchange between components of the climate system as e g. the atmosphere, the hydrosphere and the biosphere is essentially determined by the water cycle. The horizontal as well as the vertical water vapor transports contribute significantly to govern this cycle.

Water vapor is the most important greenhouse gas influencing the radiative transfer on a global scale. The knowledge of water vapor concentrations and variations in response to processes as global warming or changes of the vegetation are important for model computations of the climate. Global models on the other hand need to parameterize the moist processes as evaporation from the surface, cloud formation and precipitation which themselves act on regional scales. Improper understanding of these regional-scale processes, doubtless will cause uncertainties in the parameterization for global models.

As a consequence to these most urgent scientific questions, improved observational techniques are needed for high resolution water vapor observations in the mesoscale as well as in the global scale. Global-scale observations which only will be possible from space platforms, need proper preparatory programmes including calibration and verifications from ground (NASA, 1991). Such preparatory measurements further should improve the understanding of boundary layer meteorological processes, which influence the upscaling from small scales near the surface to scales comparable with pixel sizes as observable from space and as comparable with grid sizes of climate models.

It was one of the aims during the field experiment CLEOPATRA 1992 (Meischner et al., 1993), to improve remote sensing methods from ground, aircraft and space to observe and measure elements of the hydrological cycle.

Two quite different but complementing methods were applied and intercompared to determine water vapor structures in the atmosphere. One method was based on a multifrequency microwave radiometer system operating from ground, designed, constructed and operated by the Institute of Radioengineering and Electronics of the Russian Academy of Sciences (IRE-RAS). This system is similar to a system which will fly on PRIRODA, an earth observation module, to be docked to the Russian space station MIR end 1995 (Armane, 1991).

The other one was based on an airborne near-infrared Differential Absorption Lidar (DIAL), designed and operated by the DLR, Institut für Physik der Atmosphäre (Ehret et al., 1993). It was flown above the site of the Russian radiometer system.

Measurements will be described and discussed for three days of quite different atmospheric water vapor contents and structures. Further measurements by radiosondes and in-situ airplane methods are used for intercomparisons.

This paper is organized as follows: Next, the measurement principles and methods will be described for both systems. Paragraph 3 then describes the observational strategy, the measurements and the meteorological conditions for three selected days May 22, May 29 and June 1, 1992. In paragraph 4 the results are discussed, followed by the conclusions in paragraph 5.

2 Methods

2.1 The Microwave Radiometer Measurements

The passive microwave method is based on measurements of the microwave emission of the atmosphere at different frequencies and uses the relationships between the brightness temperature and atmospheric parameters. The relation between the brightness temperature and the meteorological parameters is described by the equation of radiation transfer inlcuding the absorption and scattering coefficients which are dependent e.g. on temperature, humidity, pressure, and drop size distributions. The principle of solving the inverse problem makes use of the relations between the brightness temperature and the meteorological parameters and of the fact, that oxygen, water vapor, clouds, rain and other atmospheric components have different spectral behaviour of emissions. Different methods of solving the inversion problem are used depending on the type and relations between the brightness temperature of the atmosphere and its components as total water vapor mass, total liquid water content in clouds, rain rate intensity and turbulence characteristics. Some methods are described in Kutuza, 1974; Petrenko, 1991; and Smirnov, 1984. Most recently a radiative-transport model has been developed by Bauer and Schlüssel (1993), to study the emitted radiaton from variable cloud and rain systems over sea using the channels

19, 22, 37 and 85 GHz of the special sensor microwave imager (SSM/I). The model, based on the matrix operator method takes into account multiple scattering and polarization. A recent review on microwave radiometric sensing of the atmosphere from ground as well as from satellites is given in M. A. Jansen (1993).

The atmospheric windows at wavelengths from 0.4 cm to 0.27 cm (ν = 75–110 GHz) or from 1.0 cm to 0.75 cm (ν = 30–40 GHz), and the resonance zone near 1.35 cm (ν = 22.235 GHz) are best suited for liquid water and water vapor measurements. Considering that the atmospheric absorption is small ($\tau(\nu) < 1$) in this spectral regions, the brightness temperature for the downwelling radiation can be approximated by

$$T_b^{\downarrow}(\nu) = T_{av}(1 - e^{-\tau(\nu)}) \quad (1)$$

with $\tau(\nu)$, the total absorption in the atmosphere, $T_{av} = T_0 - \Delta T$ the average absolute temperature of the atmosphere, T_0 the temperature at the earth surface. ΔT is the correction for a nonisotermal atmosphere depending on the frequency, the zenith angle and the meteorological conditions. ΔT varies between 5 and 20 K.

The total atmospheric absorption is given by its components of oxygen, water vapor and cloud water (Eq. (2)):

$$\tau(\nu) = \tau_{0_2}(\nu, T_0) + k_\rho(\nu, T_0)\, Q + k_\omega(\nu, T_{cl})\, W \quad (2)$$

where k_ρ and k_ω are the partial absorption coefficients of water vapor and cloud water, Q is the total water vapor mass in the atmosphere (g/cm^2), W is the integral liquid water content of the clouds (kg/m^2), T_{cl} is the effective temperature of the clouds and $\tau_{0_2}(\nu, T_0)$ is the total absorption in oxygen which may be considered to be constant.

Measurements at two or more frequencies under simplifying assumptions allow to obtain a set of equations which are linearly related to the unknown total water vapor mass Q and the liquid water content W, and nonlinearly to the unknown effective temperature of the clouds T_{cl}. The simpliying assumptions are that the dependence of τ on the real atmospheric profiles of temperature, water vapor and liquid water is neglected.

Three frequencies then are needed for the determination of this three parameters. When the temperature of the clouds is known, the brightness temperatures at two frequencies are sufficient for estimating Q and W. The spectral region near 0.33, 0.81 and 1.35 cm wavelengths are used for this purpose.

Table 1 Characteristic of the microwave systems.

Microwave receivers				
Frequencies, GHz	90	37	22.2	13.3
Wavelength, cm	0.33	0.81	1.35	2.26
PRF, GHz	2	0.6	0.6	0.6
Sensitivity, K	0.17	0.1	0.1	0.1
Polarization	V	V	V	H/V
Antennas				
Aperture, cm	9.5	30	30	15
Beam width, deg	3.5	2	3	3
Sidelobes, dB	– 18	– 18	– 18	– 13

Fluctuations of atmospheric emissions are caused by variations of the meteorological parameters as temperature, liquid water content, humidity, phase structure, etc. Such variations are further caused by turbulent motions in the troposphere. The structure function describing the atmospheric fluctuations can be estimated by these radiometer measurements too, see Gagarin and Kutuza, 1983.

The radiometers as used on ground operating at 0.33, 0.81, 1.35 and 2.26 cm wavelengths resemble those which will fly on PRIRODA. Except for the 2.26 wavelength, they were mounted on a turntable such that scanning in azimuth and elevation as well as manual scanning was possible.

The wavelengths 0.33 and 1.35 cm are mainly used to sense the moisture fields whereas for estimation of liquid water content in clouds and precipitation the wavelengths 0.81 and 1.35 cm are more appropriate. The wavelength of 2.26 cm additionally was used to estimate rain intensity by polarization measurements (see Smirnov et al., this issue).

The main characteristics of the microwave radiometer system are summarized in Table 1.

The output signals of the radiometers were multiplexed and converted into digital signals by analog to digital converters (ADC). The data rate was to be changed by software. In this experiment we used approximately 1 byte from each channel per s. The turning platform was steerable for scanning in both azimuth and elevation and allowed to make measurements of the emission in five main modes: fixed direction observation (Fix), Azimuth scan with fixed elevation (A-scan), Elevation scan with fixed azimuth (Z-scan), calibration with step by step measurements in 5–8 elevations (Calibration) and

manual positioning in any direction (Manual). The speed of rotation was adjustable between 2 deg/s and 0.25 deg/s.

The observations were made mainly in the Fix and A-scan modes. For cloudless conditions, calibrations were performed up to six times per day in the calibration mode. Most of the measurements were performed at azimuth directions between north and east at elevation angles of about 30–60°.

The data evaluation comprises two steps as described in more detail in Smirnov et al. in this volume. The first step relates values of the parameters T, Q and W to brightness temperatures by model calculations in dependence of wavelength and elevation angle. The measured relation is optimized by a least squares fit and a calibration is performed using measurements with a known temperature and humidity profile under cloudless conditions. The actual measurements in terms of radiometer output signals then are fitted to that curve (Petrenko, 1991).

2.2 Aerosol and Water Vapor DIAL Measurements

The remote measurements of an airborne near-infrared Differential Absorption Lidar (DIAL) system have been utilised for aerosol and water vapor mapping of the Planetary Boundary Layer (PBL) during the CLEOPATRA '92 field experiment. For this task, a DIAL system designed and operated by the DLR (Ehret et al., 1993) was mounted downward looking on board the Falcon meteorological research aircraft of the DLR (Fimpel, 1987).

Previous experimental studies have demonstrated the potential of the DIAL method applied in the near infrared at 720 nm to investigate water vapor distributions in the PBL either from the ground (Cahen et al., 1982, Senf and Bösenberg, 1994) or from an airborne platform (Ehret and Renger, 1990).

The DIAL technique is based on a two-wavelength lidar sounding using narrow-band laser transmitters. The so-called 'on-line' lidar measurement is related to the unknown atmospheric water vapor distribution. Typically, this measurement performed at the peak of a suitable water vapor absorption line causes an extinction enhancement of the penetrating laser beam. A second 'off-line' lidar sounding performed in the wing of the selected water vapor line serves as a reference measurement with only small or negligible absorption. This latter measurement basically relates to aerosol backscattering and extinction as known from conventional backscatter lidar techniques. From both on- and off-line measurements and known line parameters, range-resolved water vapor densities can be determined without any calibration or re-calibration procedure using the DIAL equation (R. M. Schotland, 1974) given below. The corresponding molecular absorption cross sections as a function of height can be derived by a Voigt profile calculation using standard temperature and pressure profiles known from climatological studies. Typical molecular cross sections in the 720 nm wavelength region range between 10^{-23} and 10^{-22} cm^2 as derived from laboratory measurements by different groups (Wilkerson et al., 1979, Grossmann and Browell, 1989). Previous theoretical studies have shown that absorption cross sections of $\sim 2 \times 10^{-23}$ cm^2 are adequate for DIAL measurements in the PBL (Ismail and Browell, 1989). A further criterion for correct line selection is attributed to a small temperature sensitivity of the corresponding absorption cross section to minimize errors that can arise from insufficient knowledge of the real temperature profile (Browell et al., 1991). Because of the narrow-band water vapor absorption lines with Doppler- and pressure broadened line widths of ~ 0.01 nm (FWHM) full width at half maximum, the bandwidth of corresponding laser transmitter and its wavelength stability should be in the order of ~ 0.001 nm for measurements in the lower troposphere to avoid systematical errors in the determination of the molecular absorption cross section. In addition, almost all of the laser beam energy (> 99.9 %) has to be concentrated within the narrow-band laser line in order to avoid spectral limitation or spectral purity errors in the DIAL data reduction using the conventional DIAL equation (Ismail and Browell, 1989).

The laser transmitter of the DIAL system used in this study consists of a narrow-band tuneable dye laser pumped by a frequency-doubled Nd: YAG laser. A careful recent analysis of the laser spectral profile indicated that the central peak of the dye laser is accompanied by additional unwanted broad band background emission (Ehret et al., 1993). Only about 75 % of the total energy of the present dye laser system can be kept within a spectral range of ~ 0.001 nm. The additional spectral impurity has to be taken into account in the determination of the above mentioned absorption cross section. Because of an alteration of the laser spectral profile caused by water vapor absorption, when the laser beam penetrates successive atmospheric layers, a range-dependent absorption cross section has to be taken

into account for accurate DIAL data reduction. For this task, the laser spectral profile has to be measured during the DIAL measurement, which was not the case in this study. The absorption cross section of the selected water vapor line used in the calculations in section 3 was therefore determined from a comparison with aircraft in situ measurements. A more detailed technical description of the DIAL system can be found in Ehret et al., 1993.

Close to the begining of each measurement cycle, the on-line wavelength was adjusted to maximum absorption of the selected water vapor line by use of a photo acoustic cell. During the DIAL measurements the laser wavelength was repetitively multiplexed between on- and off-line at a rate of ~ 8 Hz. The photons scattered back from the atmosphere are collected by a 35 cm diameter cassegrainian-type telescope, passing a ~ 0.6 nm (FWHM) spectral filter and are finally detected with a photomultiplier. The lidar signals are digitized with a resolution of 12 bits at a sampling rate of 10 MHz, which corresponds to a vertical resolution of 15 m in the lidar retrieval. From both on- and off-line lidar backscatter returns $P_{on}(R)$ and $P_{off}(R)$, the mean water vapor particle number density $N_{H_2O}(R)$ of the range cell ΔR at a distance $R = R_1 + \Delta R/2$ can be calculated with the DIAL equation:

$$\overline{N}_{H_2O}(R) = \frac{1}{2\sigma_{eff}\Delta R} \ln \frac{P_{off}(R_2)\, P_{on}(R_1)}{P_{on}(R_2)\, P_{off}(R_1)}$$

where σ_{eff} is the effective absorption cross section of the selected water vapor line, as mentioned above. For the measurements presented, ΔR has been set to 300 m. The water vapor mass mixing ratio m (in g/kg) is obtained from the following equation: $m = 0.22\, N_{H_2O}(R)/N_{air}(R)$,: with $N_{air}(R)$ being the particle number density of dry air at the distance R, usually taken from standard atmospheres.

The precipitable water w_p (in kg/m^2) is obtained from the DIAL measurements by integrating the particle number density over the height, from $h_0 = 1$ km to $h_1 = 2.5$ km, and multiplying with the mass of a water molecule m_{H_2O}:

$$w_p = m_{H_2O} \int_{h_0}^{h_1} N_{H_2O}(h)\, dh$$

Due to the range cell size ΔR of 300 m, the DIAL measurements only cover the altitude range between 1000 and 2500 m. They have been completed by radiosonde data in order to get a value for the total water vapor column of the troposphere. The exact ground altitudes were available from the lidar measurements. The total water vapor content for each flight leg was then plotted as space series along the path. Because the aircraft speed was much higher than the windspeed, Taylor's hypothesis of a 'frozen atmosphere' can be applied and the plots can be regarded as showing the state of the atmosphere at a particular time.

For each such total water vapor content series, the ratio (standard deviation)/(mean value), known as variation coefficient, has been determined. It represents the sum of natural variations as well as statistical errors and lies between 9 and 14 %. The variation coefficient represents an upper limit for the statistical error. Given the fact that natural variations always exist, the statistical error is expected to lie well below this limit. The use of a standard atmosphere particle number density profile instead of the real unknown profiles leads to an estimated additional error of at most 5 % for the total water vapor content.

3 Observations

3.1 Experimental Set Up

The measurements were embedded into the overall observational net of CLEOPATRA (Meischner et al., 1993, The strategy was to fly cross sections with the DIAL system onboard the FALCON research aircraft (Fimpel, 1987) just above the measurement site of the microwave radiometer system. In situ humidity values measured by the aircraft during ascent and descent were used for the determination of local humidity profiles in addition to the Munich radiosonde, about 50 km north of the measuring site. The planned flight pattern centered above the Lichtenau, the sight of the radiometers, is shown in Figure 1. The flights were planned in accordance to the weather situations and the availability of observational systems. The microwave radiometers mostly measured in northern and northeastern azimuth and at an elevation angle between 30° and 60°.

3.2 Measurements on May 22

On May 22, 1992, a high pressure system extended from the Balkans to Great Britain and Scandinavia. The dominating high centered over northern Scandinavia intensified and spread out southeastwards. Southern Germany was situated at the southwestern edge of this high pressure system. A continental, dry, moderate easterly airflow was observed at all levels. The pressure distribution was indicative for

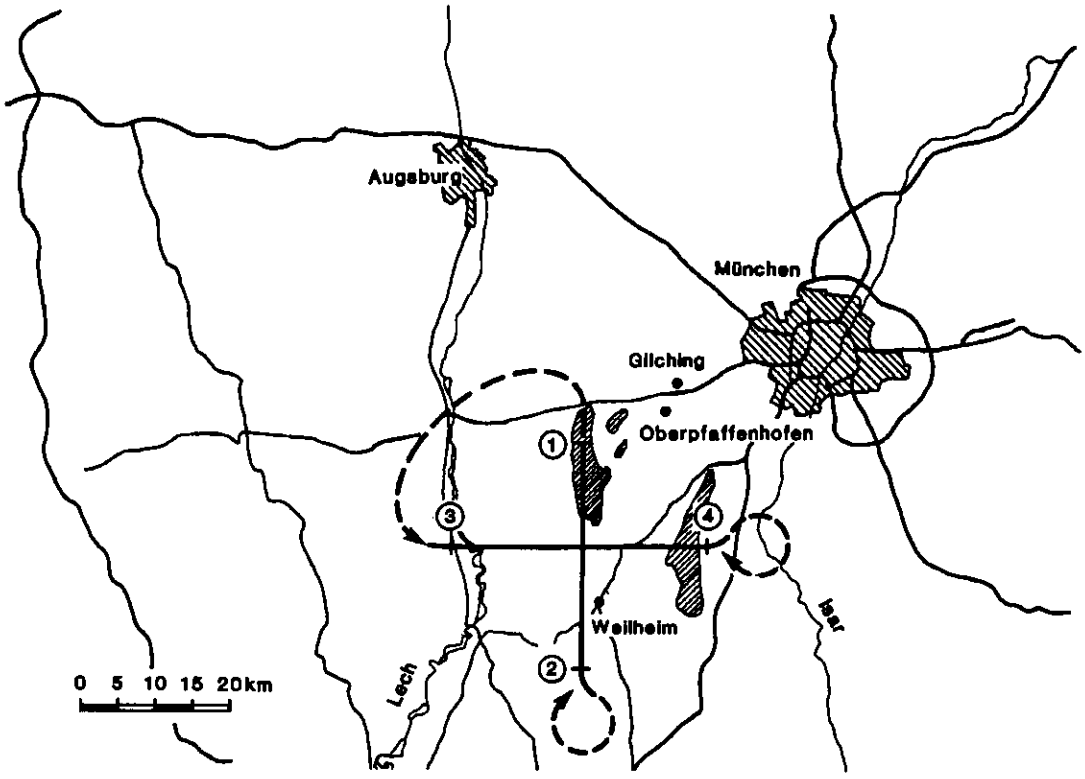

Figure 1 A cross-shaped pattern was flown above the site of the microwave radiometer system (center of the cross). The measurements were imbedded into the overall CELOPATRA observational area (Meischner et al., 1993). The numbers indicate start and end points of the aircraft measurements.

stable calm weather during the whole day. The southeasterly winds further showed that a depression over the eastern Atlantic was not to influence the weather in southern Bavaria, as well as the local low observed over the western Alps. A tenuous scattered cirrus veil in the upper atmosphere of the measurement area was detected in the NOAA-AVHRR-scene at 0710 UTC (not shown) which corresponds to the time of measurements. This may origin from the local Alpine low pressure system which extended from the surface to the tropopause. Except of these thin upper level clouds, southern Bavaria was cloudless as confirmed by observations from Deutscher Wetterdienst.

The nocturnal inversion only reached 270 m height above ground. During daytime the air dried out. The cold air descended under the high pressure influence, thus limiting convective activity. The subsidence of the dry continental air mass caused a stable stratification of the atmosphere.

The precipitable water at 12 UTC was about 30 % below the value of midnight (radiosonde Munich 00 UTC: 13 kg/m^2, 12 UTC: 10 kg/m^2). About 90 % of the total water vapor content of the atmosphere was concentrated below 4 km, the flight level of the Falcon for the DIAL measurements of this day.

Figure 2 shows the water vapor mixing ratio (equivalent to the specific humidity) from the Munich radiosonde at 00 and at 12 UTC. The measurements of the morning flight of the Falcon are added. These were measured during ascent and descent thus having a time difference of one hour. A comparison of both radiosonde profiles shows that still dryer air is advected during daytime in a level between 2 and 4.5 km altitude. The data from the Falcon ascent and descent agree, indicating that there is no remarkable change within that one hour. The maximum difference is 0.3 g/kg, probably due to some convection which is limited in depth during the early morning. A comparison of the Falcon data and the Munich radiosonde data shows a difference of up to 0.7 g/kg in the water vapor mixing ratio, which represents the temporal and spatial variability of water vapor distributions under this weak wind condition.

The precipitable water as derived from the DIAL measurements between 0700 and 0735 UTC and complemented by the radiosonde profile in order to

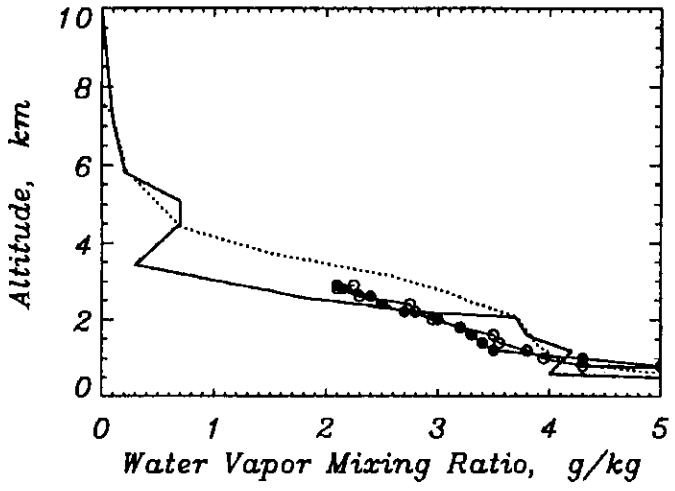

Figure 2 Water vapor mixing ratio profiles from the Munich radiosonde on May 22, 1992 at 00 UTC (dotted) and 12 UTC (solid). The data of the aircraft ascent are from 0650 to 0653 UTC (circles) and of the descent from 0743 to 0751 UTC (dots).

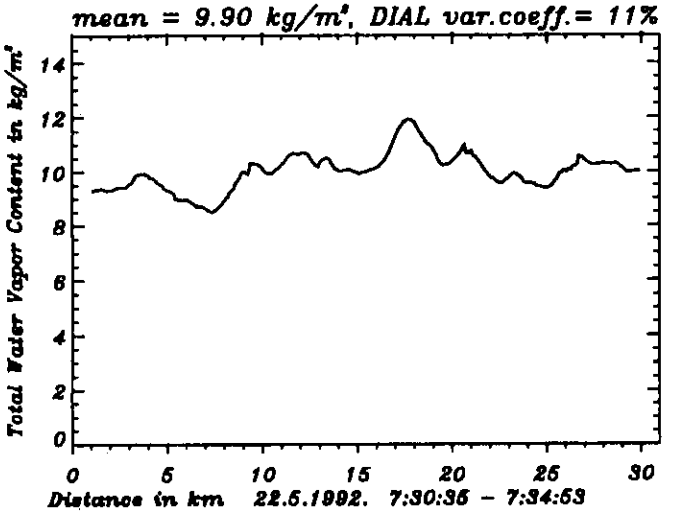

Figure 3 Precipitable water as obtained by DIAL measurements on May 22, 1993. This horizontal profile was measured along the flight track (3) to (4) of Figure 1. The series mean value and variation coefficient are given at the top of that plot.

cover the whole atmosphere, ranges between 8 and 12 kg/m^2 with a mean value of 10 kg/m^2. As an example, Figure 3 shows the precipitable water along the west-east flight leg (see Figure 1). The variations observed represent the actual fluctuations in the atmosphere. An influence from surface characteristics has not been found.

A time series plot of the precipitable water as derived by the radiometer system is shown in Figure 4. It covers a time period of 50 min including

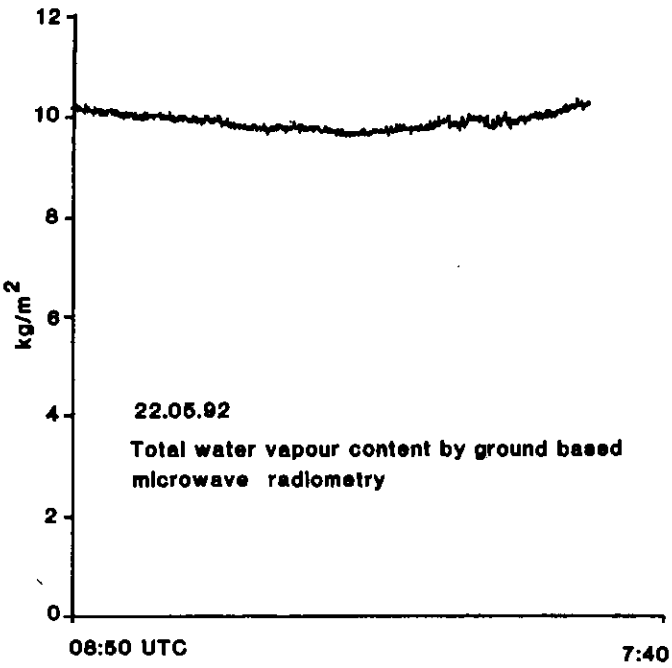

Figure 4 Time series of precipitable water, as measured by the multifrequency microwave radiometer system on May 22, 1992, 0650 UTC - 0740 UTC.

the time of the DIAL measurements. The mean value of 10 kg/m^2 agrees excellently with these. The radiometer time series further represents the calm and only slowly changing situation.

3.3 Measurements on May 29, 1992

On May 29, 1992 a transient high between a low, west of France and a low over Rumania determined the weather in southern Germany. At 00 UTC strong northwesterly winds at the upper levels indicated, that Munich was still at the cold side of the Rumanian low while at 12 UTC the southwesterly winds showed that the upper level now was influenced from the warm side of the France low. Indeed the temperature increased within that 12 hours by 2 K at the 400 hPa-level. The warm moist air was advected above an altitude of 6 km. But this moist upper air mass only contributed to less than about 10 % to the total water vapor content of the troposphere. Below 6 km, there was a very dry air mass, separated from the moist air by an inversion which descended by about 1 km from midnight to noon indicating the approaching warm front (Figure 5). This calm and very dry air mass extended from 2 to 6 km altitude. Several moist layers of only some hundreds meters in depths were embedded. The winds there were very weak, thus, the advection was low between 2 and 6 km height. Below the inversion in 2 km altitude, a steady

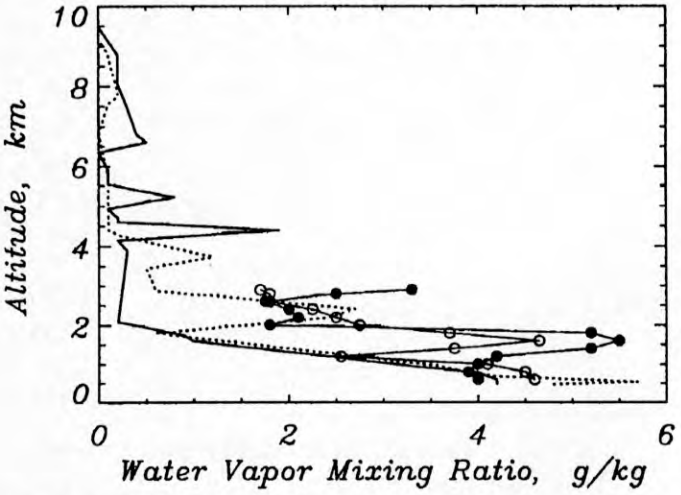

Figure 5 Same as Figure 2, but on May 29, 1992. The Falcon ascent was between 0654 and 0658 UTC, the descent between 0822 and 0829 UTC.

layer. Such a low level jet often occurs in transient hight pressure weather situation north of the Alps.

Thus, the whole atmosphere at that day showed a rather inhomogeneous structure. In the upper level the moist air already arrived from south-west, while in the low level the dry continential air remained blowing from the east for several days and getting dryer from day to day. Since the lower levels contribute most to the precipitable water of the troposphere, the total value was even less than for the dry May 22 as shown above. It was only 7 kg/m^2 at night and 5 kg/m^2 at noon.

Water vapor measurements on this day were performed only by the DIAL system. The Falcon was operating performing measurements according to Figure 1 between 0700 and 0830 UTC in the morning. During that time eight cross sections were

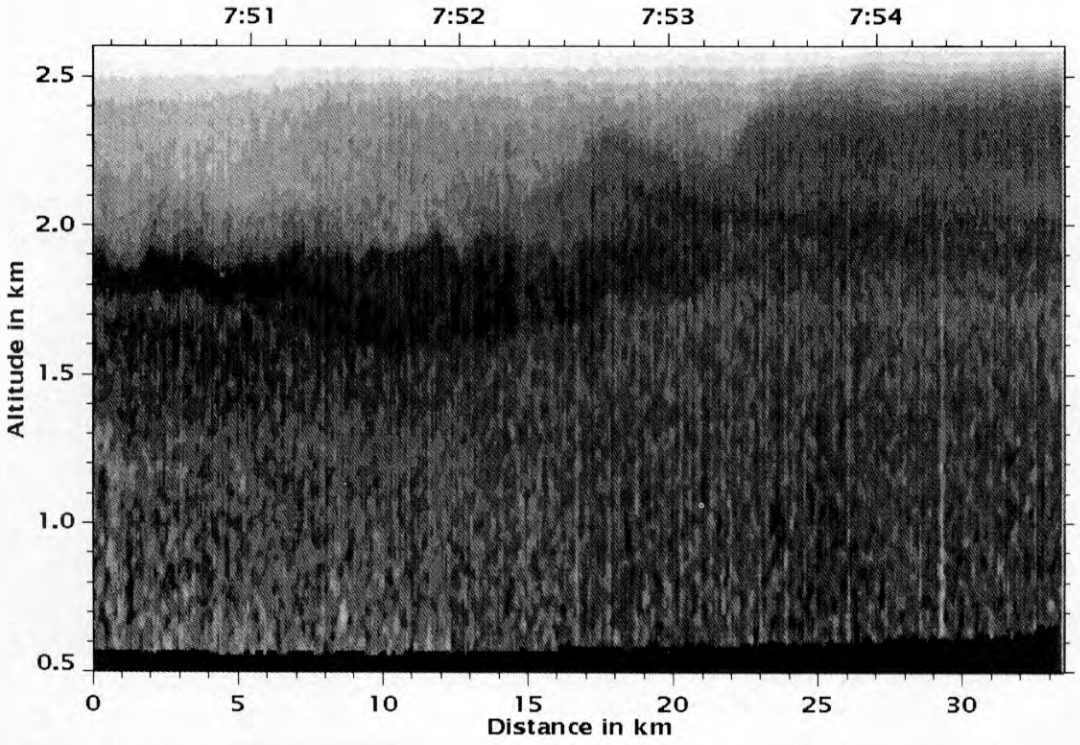

Figure 6 Vertical cross section of the atmospheric aerosol backscattering along the north-south leg on May 29. The linear grey backscatter-intensity scale goes from black (strong) to white (weak backscattering). The strong black line at the bottom is the ground signal. Atmospheric layers indicated by different backscatter intensities can be detected. The free atmosphere is characterized by weak backscattering and extends above around 2 km altitude.

decrease of the humidity with altitude was observed and the relative humidity at ground did not exceed 70 % at night or 50 % at day. In the lowest two km of the atmosphere easterly winds were predominant. Near to the Alps increased speeds up to 12 m/s at night and up to 7 m/s at day were observed in that

flown covering each of both legs of the cross twice in each direction. Figures 6 to 9 in an exemplary way present one aerosol backscatter and one water vapor vertical cross section for each leg. The two-dimensional aerosol backscatter measurements are essential for visualization of the structure and the

state of the boundary layer. They especially show inhomogeneities which otherwise by e.g. radiosoundings will not be detectable. Thus misinterpretations will be reduced. Figure 6 shows the aerosol backscatter intensity for the north-south leg starting at point 1 above the lake Ammersee. The lake extends to km 12.5. The boundary layer is characterized by a higher aerosol concentration than the free atmosphere above. It reaches an altitude of 2000 m above the plain and extends to 2.5 km in the south above the Bavarian prealps, around km 30. Above the lake up to an altitude of 1300 m the aerosol backscatter intensity clearly is somewhat weaker than above the land. The strong aerosol backscattering near the inversion layer between 1800 and 2000 m altitude is because of aerosol swelling in regions with increased relative humidity.

Figure 7 shows a vertical cross section of the water vapor mixing ratio along the same track as in Figure 6. We note that the originally strong water vapor gradients have been smoothed to some extent by the applied smoothing algorithm used to reduce the noise-induced statistical error. The statistical error has been determined to be less than 0.2 g/kg. Above the lake, the water vapor concentration of up to 8 g/kg very impressively shows values four times higher than above land, within the boundary layer up to 1300 m altitude. The weak easterly winds do not influence the impressively exact coincidence of the strong horizontal water vapor gradient with the southern lakeside at km 12.5. Between 1300 m altitude and the inversion at around 2000 m a humid layer extends over land with mixing ratio values ranging from 5 to 7 g/kg. The lake clearly is represented as a strong water vapor source. The moisture flux originating from the lake goes up to the inversion layer and then expands horizontally below the inversion.

This impressive correlation with the location of the lakes can be explained by several facts:

Firstly, at the time of measurement in the morning, the land surface was not yet heated, thus giving very low evaporation rates. The water on the other hand was warmed up during the long period of warm and sunny weather. Because of the very dry air near the ground, the evaporation-caused humidity above the lakes in the morning was several times higher than the values of the general environmental air.

Secondly, a very calm situation in the morning did not disturb this pattern neither by advection nor by convection. And thirdly, the boundary layer in the area of measurements was homogeneous with height, thus enabling the moisture fluxes to extend up to its

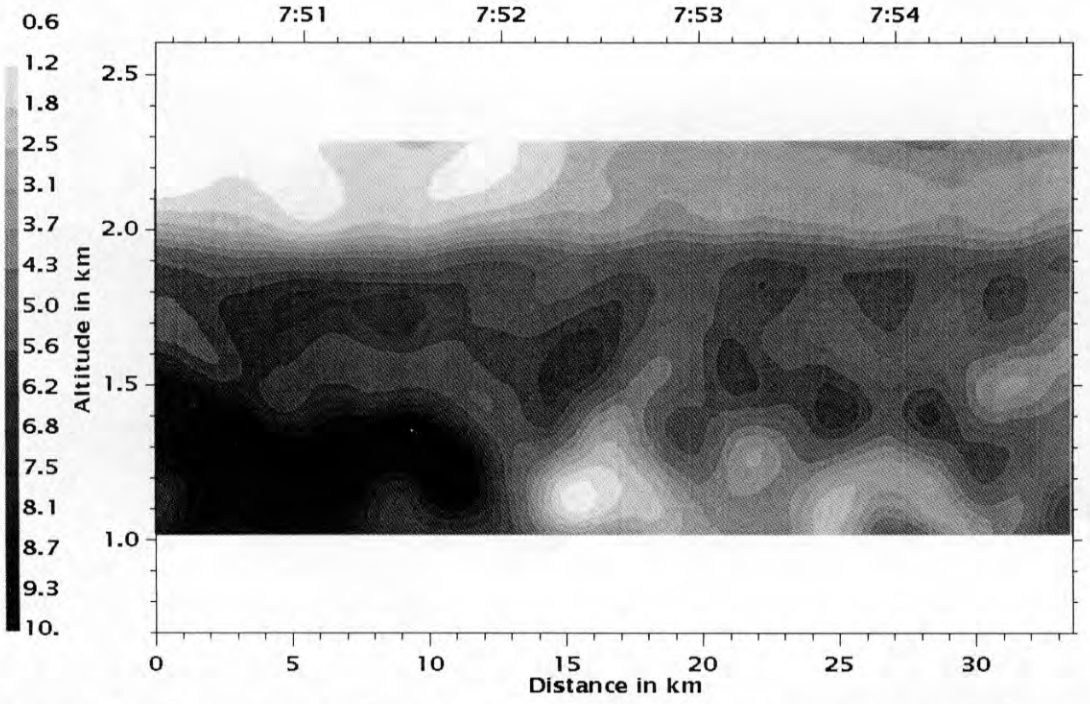

Figure 7 Vertical cross section through the atmosphere of the water vapor mixing ratio along the north-south leg on May 29. The grey scale indicating the mixing ratio in g/kg is given at the left. The bubble structure comes from the fact that the data have been smoothed horizontally by 3 km and vertically by 300 m.

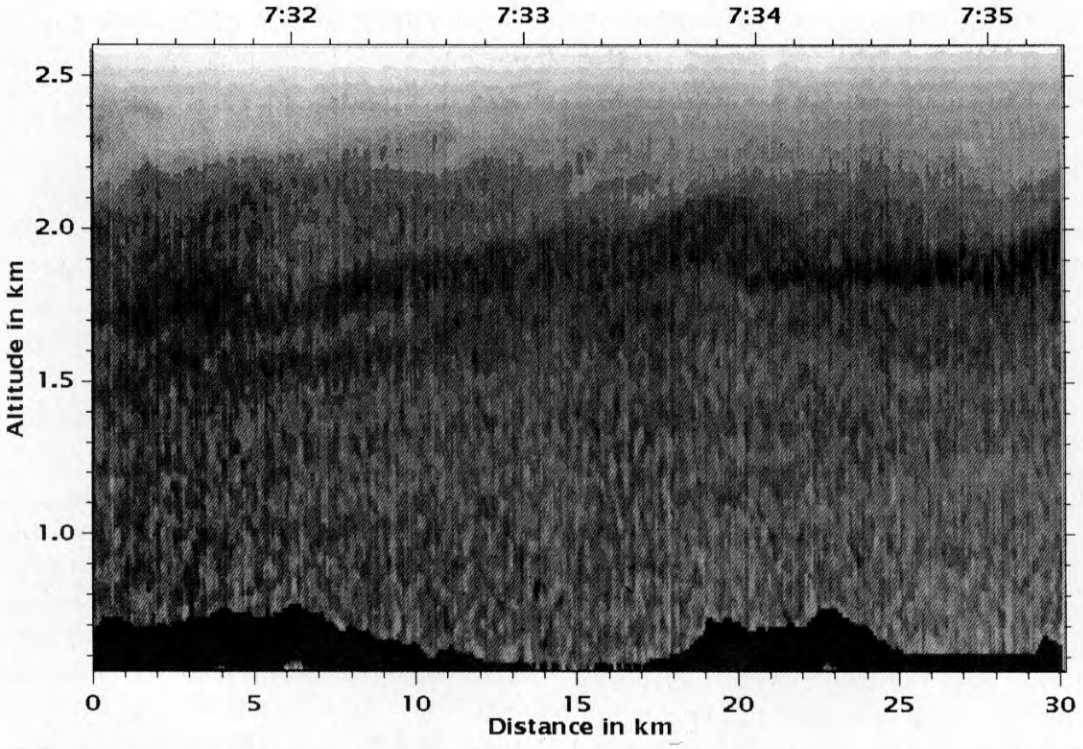

Figure 8 Aerosol backscatter cross section along the west-eat leg on May 29. Same representation as Figure 6.

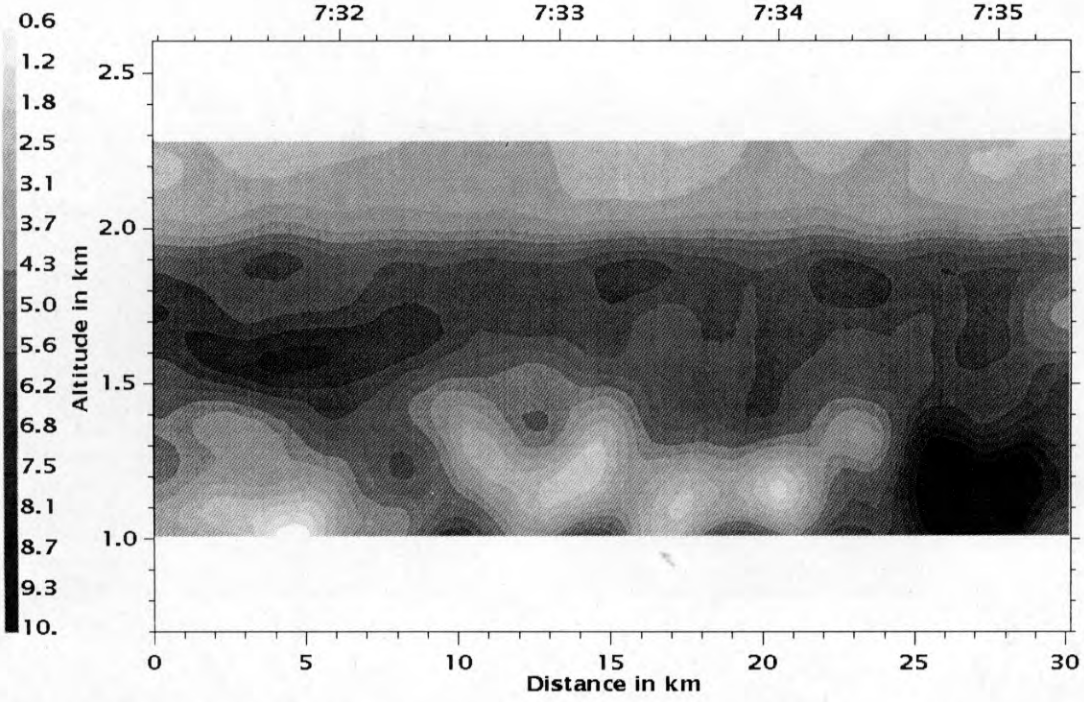

Figure 9 Water vapor mixing ratio cross section along the west-east flight leg. Same representation as Figure 7.

top. On May 22 under similar conditions a weak near-surface inversion in about 650 m altitude was observed, possibly preventing a uniform moisture flux up to the ABL top.

Above the inversion the water vapor mixing ratio variations correspond to the structure of the boundary layer (see Figure 6). From km 25 southwards, mean increased values of the mixing ratio lie around 3 g/kg between 2100 and 2500 m altitude in accordance with the elevated boundary layer there. The mean value of the moisture content of the free atmosphere for the same altitude region above the lake (km 0–km 20) lies around 1 g/kg.

The aerosol backscatter situation for the west-east leg from point 3 to point 4 is given in Figure 8. The boundary layer depth goes up to 2000 m, again with aerosol swelling just below the inversion between 1700 and 2000 m altitude. In the eastern part, between km 25 and km 29.5, the lake of Starnberg was overflown as can be seen by the flat horizontal surface. The corresponding water vapor cross section, Figure 9 clearly shows again that the lake acts as a source of water vapor. At the center point of the flight pattern cross (Figure 1), the measurements of both cross sections agree well. This point lies at km 18 for the Figures 6 and 7 and at km 15 for Figures 8 and 9.

3.4 June 1, 1992

On June 1st, a low pressure system near Iceland and high pressure over Scandinavia did determine the weather in southern Germany. A short-wave minor trough crossed France at the warm side of the Iceland low which transported humid subtropical air with southerly winds into the measurement area. This slow minor trough caused a weak lifting of the air initiating convective activities, partly with vigorous showers and thunderstorms over southern Bavaria. These clouds were observed by the NOAA5 AVHRR images (not shown) and from ground. A surface depression with small pressure gradients and associated weak winds was located over western and southern Germany at 12 UTC. The noon radiosonde ascent of Munich showed weak southwesterly winds at all levels. The strong surface heating caused convection which deepened during the afternoon. At low levels the temperature and the moisture were high to initiate convection. During the whole day, humid warm air from the Mediterraneum propagated with southwesterly weak winds into southern Germany, thus maintaining thunderstorm activity.

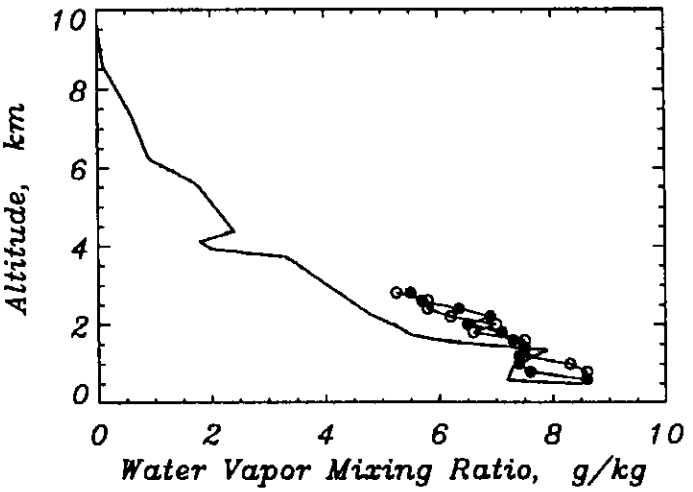

Figure 10 Same as Figure 2, but on June 1, 1992. The Falcon ascent was between 1147 and 1152 UTC, the descent between 1217 and 1226 UTC. Note the different scale for the water vapor mixing ratio as compared to Figures 2 and 5.

The precipitable water was 22 kg/m^2 at noon as determined from the Munich radiosonde. This was about twice the value observed on May 22. On June 1st, about 80 % of the total water vapor mass was concentrated below the Falcon flight altitude of 4 km on this rather moist day.

Figure 10 shows the water vapor mixing ratio from the radiosonde Munich at 12 UTC and the Falcon data measured between 1147 and 1226 UTC.

Although the time difference between the Falcon ascent and descent is only 40 minutes, the corresponding water vapor mixing ratios differ up to 1 g/kg which is about 10 % of the ground level values or about 20 % at 3 km altitude. Because of the weak advection on this day, these differences indicate small scale time variations of the water vapor concentrations caused by convection. A comparison of the Falcon data with the Munich radiosonde brings up still greater differences. The aircraft measurements show up to 1.4 g/kg higher values. The most pronounced deviations between the radiosonde data and the airborne data were found near the surface and near an altitude of 2.3 km which is the cumulus cloud level. In general, the relative maximal differences of the mixing ratios between the aircraft measurements and the radiosonde, 50 km apart from each other are similar for both extreme situations, the dry May 22 and the moist June 1; they were about 25 %. The RMS error for the whole profile is about 10 % for both days.

The DIAL measurements on this day were performed between 1155 and 1215 UTC. The aerosol backscatter plot for one exemplary south-north leg

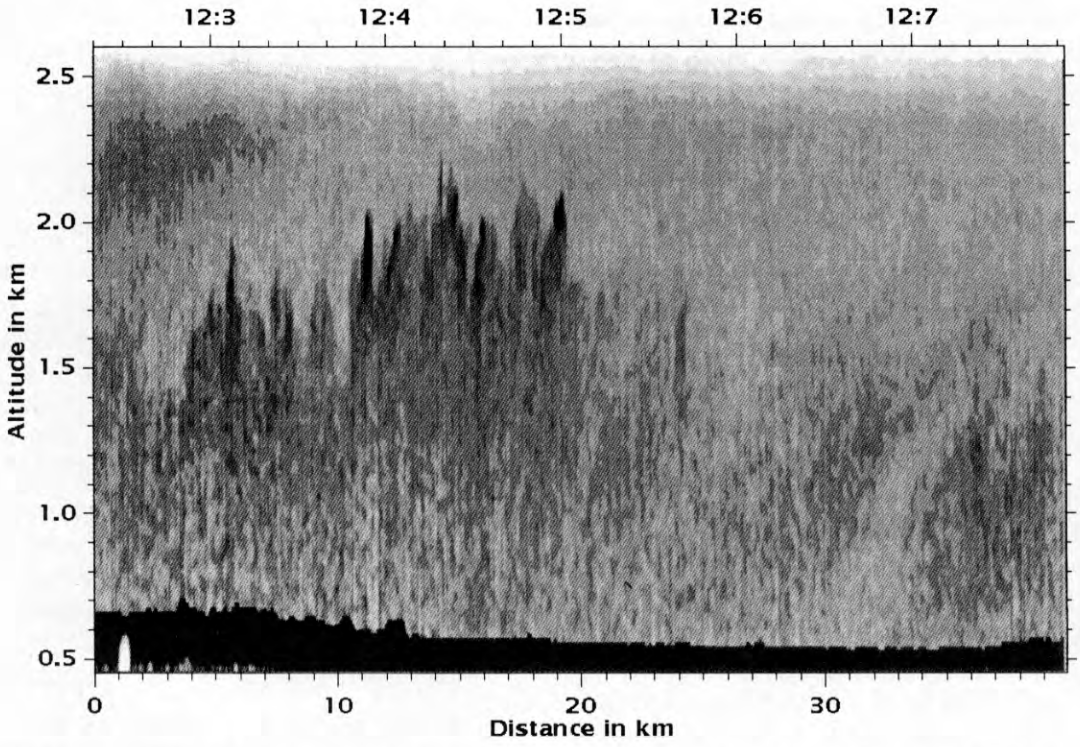

Figure 11 Aerosol backscatter vertical cross section along the south-north flight leg flown on June 1. Same representation as Figures 6 and 8.

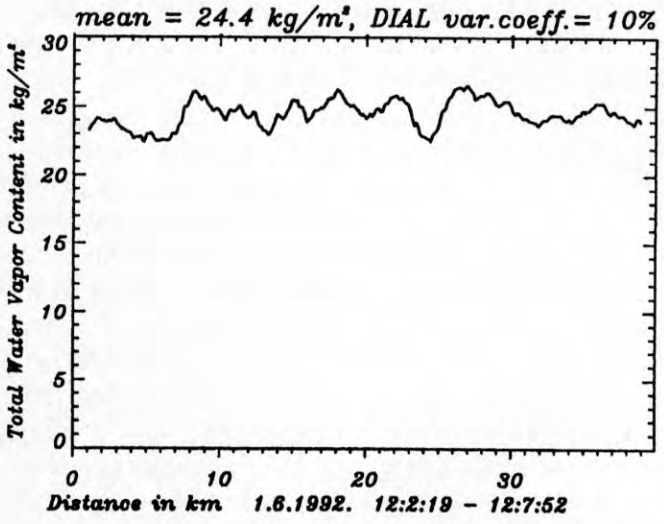

Figure 12 Precipitable water along the south-north flight leg on June 1, 1992. Same area as in Figure 11 and same representation as for Figure 3.

from point 2 to point 1 (Figure 1) is given in Figure 11. It shows a convectively mixed boundary layer with convective elements over land (in the range 0 km–30 km) rising up to about 2 km altitude. Above the lake Ammersee, between km 30 and km 37, the convection clearly is seen to be small at this time.

The profile of the total water vapor content along that flight leg as shown in Figure 12 does not reveal any significant correlation with the lake area or with the convective structure. The water vapor content values lie between 22 and 27 kg/m^2, with a mean of 24.4 kg/m^2.

The microwave radiometer measurement resulted in time series which well agree with the DIAL measurements. Figure 13 shows an example for the time of the DIAL measurement. Agreement can be stated for the total values, fluctuating between about 22 and 27 kg/m^2, as well as for the degree of variations, indicating the fluctuations caused by the convection late morning of that day. A moderate increase of the precipitable water with time might be due to increasing evaporation caused by warming of the surface.

4 Discussion

The measurements of the precipitable water by four different methods – multifrequency microwave radiometry, water vapor DIAL, radiosondes and in situ aircraft measurements – for two selected days agree within the estimated measurement errors, taking into account the different time and space

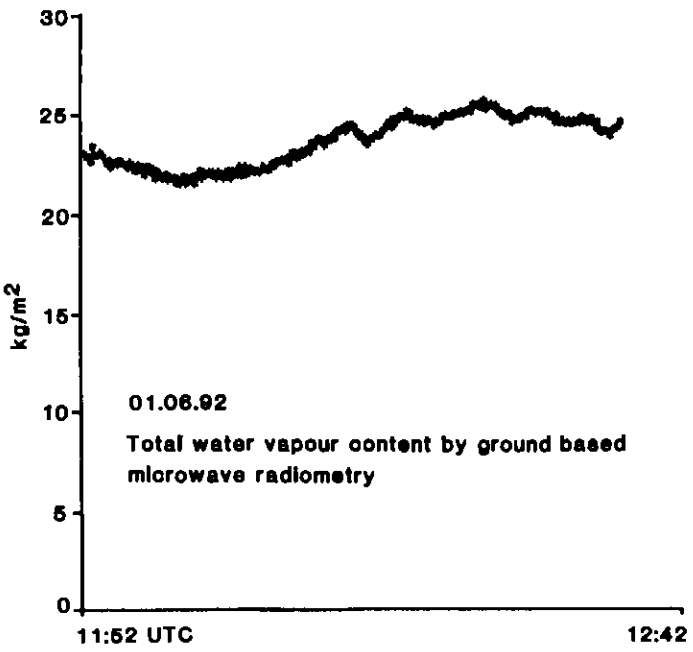

Figure 13 Time series of precipitable water on June 1, as measured between 1152 UTC and 1242 UTC by the ground based multifrequency microwave radiometer system.

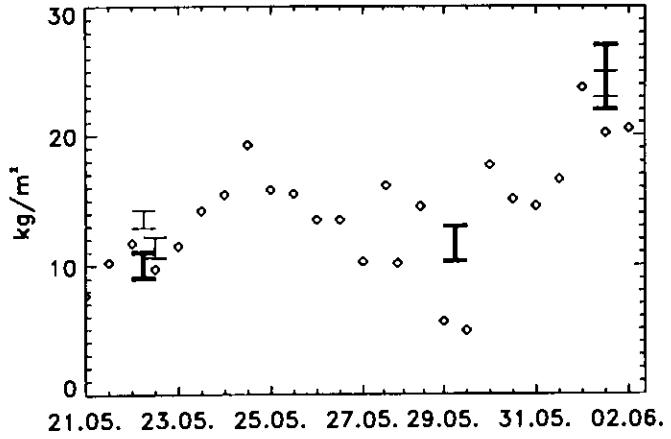

Figure 14 Overview of the Munich radiosonde data between May 22 and June 1 (diamonds). The strong error bars on May 22, May 29 and June 1 indicate the DIAL daily averaged values. The thinner error bars represent the radiometer measurements.

scales and different measurement locations. They verify and complement each other. The DIAL measurements give high space resolution, mapping the humidity structure and the boundary layer structure of the cross section along the flight track, whereas the microwave radiometry gives a comparable time resolution at one fixed location. The analysis of both variations, the time variation measured by the microwave system and the space variation as measured by the DIAL system may contribute for distinguishing between vertical fluxes of latent heat governed by surface characteristics and convection and large scale advection processes.

The observation of the days May 22 and June 1 show interesting differences. On May 22 the measured (DIAL) spatial variations are significantly higher than the local time variations, whereas on June 1 both, spatial and time variations show very similar behaviour. This can be explained by the neglegible dynamics and negligible convection in the morning of May 22. Further, the low wind speed explains that existing humidity inhomogeneities are not transported horizontally across the measurement site of the microwave radiometers.

The measurements of June 1st were performed around 1200 UTC. At that time convection clearly already was active and increased further during the day. The such caused humidity fluctuations are represented in space and time series equally. Because of the low wind speed similar to May 22 influences of advection can be neglected.

Measurements from the microwave radiometer system and from the DIAL system of May 22 and June 1 are shown in Figure 14. DIAL measurements are given further for May 29. They are compared with the time series of the Munich radiosonde as presented in Meischner et al. (1993).

Excellent agreement between all three measurements can be stated for the two days May 22 and June 1. Both days are characterized by rather homogeneous conditions in the mesoscale and with altitude. May 22 was a calm dry day with continental dry moderate southeasterly airflow in all levels. June 1 with weak southwesterly winds in all levels and weak lifting was characterized by convective activity during the whole day and in the whole area. This convective activity caused the higher variances of water vapor fluctuations.

Around May 29 the situation was quite different. The whole atmosphere of that day showed a rather inhomogeneous structure with dry continential air coming in from the east near ground and humid air arriving from west in upper levels with several moist layers only some 100 m in depth embedded in between. So, big differences between different measurement locations only confirm the spatial variability of water vapor structures as seen along the north-south track, Figure 15.

It is important, however, to note that the microwave radiometer measurements near the Alps not shown here, for these situations result in significant higher values than the Munich radiosonde. This difference partly might be explained by the moist air approaching at high levels from the south.

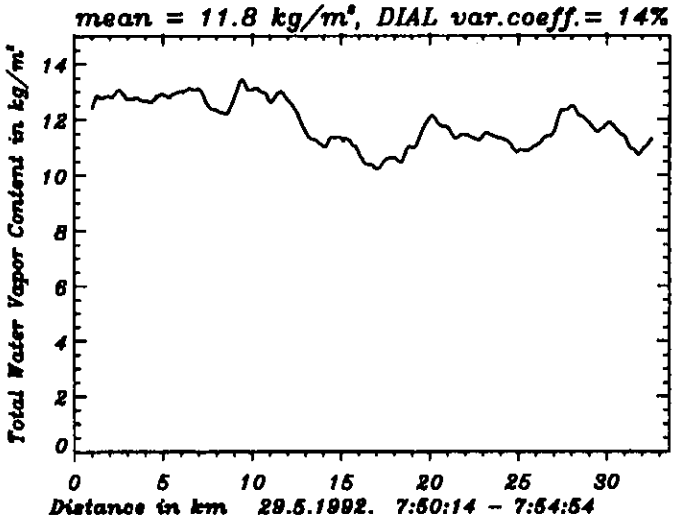

Figure 15 Precipitable water along the north-south flight leg on May 29 measured by the DIAL system between 7:50 and 7:56 UTC.

The DIAL measurements of May 29 were performed early in the morning between 0730 and 0800 UTC. Very dry air near ground determined the precipitable water to be very low, see Figure 14.

Under these calm and very dry conditions in the morning the land surface characteristics impressively map into the boundary layer. The boundary layer depth as observed by the aerosol backscattering shows elevated values above land compared to the observations over the lakes Starnberger See and Ammersee. Clearly detectable are further a lower aerosol backscatter signal across the lakes. The most impressive observations however are the enhanced water vapor concentrations, well correlated with the locations of the lakes in north-south direction as well as in west-east direction. These water vapor concentrations just above the lakes are measured to be four times higher than over land. This moisture flux from the lakes extends upwards within the boundary layer to its top, then spreading sidewards.

It is quite interesting to discuss this example via the land surface cover classification according to scale organization of surface inhomogeneities as suggested by Shuttleworth (1988). He classified land surface covers as "A", if it exhibits disorganized variability at length scales of 10 km or less, which gives no apparent organized response in the ABL.

Classification "B" is given to a land surface cover which exhibits variability, which is organized at length scales of greater than 10 km, possibly giving an organized response in the atmosphere such as to alter the effective value of surface properties.

Our case study clearly shows that the effectiveness of a response of surface variability to the atmosphere and especially the structure of the ABL further depends on conditions as humidity of the atmosphere and the inputs which influence the strength of mixing and advection.

In general our measurements show that most of the small scale variability of water vapor is averaged within the ABL. This supports the suggestion of Shuttleworth, 1988, that "the effective value of large-scale, area averaged vegetation and soil characteristics over land surfaces which exhibit disorganized variability at length scales of ten kilometers or less, may resonably be approximated by a simple average of the behaviour of different surface cover present, weighted by the fractional area populated". This finding further will simplify the upscaling problem and the use of remote sensing data from satellites for estimation of area averaged moisture fluxes.

5 Conclusions

It has been shown that multifrequency microwave radiometry as well as DIAL are powerful tools in monitoring water vapor structures of the atmosphere. The measurements of precipitable water agree well with each other as well as with the more conventional measurements with radiosondes and aircraft in situ measurements. DIAL and microwave radiometry complement each other ideally in time and space resolution. The microwave measurements from a fixed location can be performed with high time resolution of minutes, whereas the DIAL measurements results in space resolution of some 100 m along the flown cross section. Proper analysis of combined measurements comparing time and space series enables to distinguish between advection and convection processes.

Both remote sensing methods are qualified to operate from space but both need verification and validation from the ground. The DIAL technique has the advantage that water vapor profiles can be derived without any calibration procedure. However, this requires a powerful narrow-band laser transmitter possessing a very high spectral purity. System improvements concerning the DIAL technique are currently in progress and the forthcoming PRIRODA programme will give a good opportunity for further tests and applications.

Acknowledgements

The participation of IRE in the field programme CLEOPATRA as a preparatory step towards the PRIRODA mission has been made possible by a DARA (Deutsche Agentur für Raumfahrtangelegenheiten) fund under contract FKZ 50 EE 9212. The adaptive administration of this newly established collaboration is greatly acknowledged. The operation of the microwave radiometer system at ZDBS, Lichtenau, was made possible and was supported by R. Manetsberger who always was ready to help. G. Rossmeier and R. Schöneberg typed the manuscript with great patience and G. Jacob and G. Steudel carefully prepared some of the figures. Thanks are due to all of them.

References

Armand, N. A., 1991: Orbital station "MIR", complex of remote sensing of the earth "PRIRODA", Scientific Program. Institute of Radioengineering and electronics of the USSR Academy of Sciences, Moscow.

Akriloneva, A. B., B. G. Kutuza, 1978: Microwave radiation of clouds. Radiotecknica i Electronica **23**, No. 9, 1792–1806; Radio Eng. and Electron. Phys. **23**, 12–24.

Barret, A. H., A. Chung, 1962: A method for the determination of high altitude water vapor abundance from ground-based microwave observation. J. Geophys. Res. **67**, No. 11, 4259–4266.

Bauer, P. and *P. Schlüssel*, 1993: Rainfall, total water, ice water, and water vapor over sea from polarized microwave simulations and special sensor microwave/imager data. J. Geophys. Res. **98**, No. D 11, 737–759.

Browell, E. V., S. Ismail, B. E. Grossmann, 1991: Temperature sensitivity of differential absorption lidar measurements of water vapor in the 720 nm region. Appl. Opt. **30**, 1517–1524.

Janssen, M. A. (Editor), 1993: Atmospheric remote sensing by microwave radiometry. John Wiley and Sons, Inc., New York.

Cahen, C., G. Megie and *P. Flament*, 1982: Lidar monitoring of water vapor cycle in the troposphere. J. Appl. Meteorol. **21**, 1506–1515.

Ehret, G., C. Kiemle, W. Renger, G. Simmet, 1993: Airborne Remote Sensing of Tropospheric Water Vapor Using a Near Infrared DIAL System, Appl. Optics **32**, No. 24, 4534–4551.

Ehret, G., W. Renger, 1990: Atmospheric aerosol and humidity profiling using an airborne DIAL system in the near IR, Optical Remote Sensing of the Atmospheric, Vol. 4 of OSA Technical Digest Series, 586–589.

Fimpel, H. P., 1987: The DFVLR meteorological research aircraft Falcon-E; instrumentation and examples of measured data. Sixth Symposium on Meteorological Observations and Instrumentation, January 12–16, 1987. American Meteorological Society, 113–116.

Gagarin, S. P., B. G. Kutuza, 1977: Aircraft measurements of spatial characteristics of fluctuations of atmospheric radioemission at wavelengths 0.8 and 1.35 cm. Izv. Acad. Nauk USSR, FAO **13**, No. 12, 1307–1311.

Gagarin, S. P., B. G. Kutuza, 1983: Influence of sea roughness and atmospheric inhomogenities on microwave radiation of the atmosphere ocean system. IEEE J. Ocean. Engin. **OE-8**, No. 2, 62–70.

Grossmann, B. E., E. V. Browell, 1989: Water vapor line broadening and shifting by air, nitrogen, oxygen, and argon in the 720 nm wavelength region. J. Mol. Spectrosc. **138**, 562–595.

Ismail, S. and *E. V. Browell*, 1989: Airborne and spaceborne lidar measurements of water vapor profiles: a sensitivity analysis. Appl. Opt. **28**, 3603–3615.

Janssen, M. A. (Editor), 1993: Atmospheric remote sensing by microwave radiometry. John Wiley and Sons, Inc., New York, 572 p.

Kutuza, B. G., 1974: Investigation of total water vapor content fluctuations in the atmosphere by radioastronomical method. Izv. Acad. Sci. USSR, FAO **10**, No. 11, 1148–1156.

Meischner, P., M. Hagen, T. Hauf, D. Heimann, H. Höller, U. Schumann, W. Jaeschke, W. Mauser, H. R. Pruppacher, 1993: The Field Project CLEOPATRA, May–July 1992 in Southern Germany, Bull. Amer. Meteorol. Soc. **74**, 401–412.

Meischner, P., 1993: CLEOPATRA 11.05 bis 31.07.1992. Synopse der Messungen und Ergebnisübersicht. DLR-Mitt. 93–111.

NASA 1991, The Role of Water Vapor in Climate. A Strategic Research Plan for the Proposed GEWEX Water Vapor Projekt (GVaP). NASA Conference Publication 3120, 50 p.

Petrenko, B. Z., 1991: External calibration of satellite passive microwave measurements and retrieving of geophysical parameters, Proc. IGARSS '91, Helsinki **4**, 2385–2387.

Schotland, R. M., 1974: Errors in the lidar measurement of atmospheric gases by differential absorption. J. Appl. Meteorol. **13**, 71–77.

Senff, Ch. and *J. Bösenberg*, 1994: Measurement of Water Vapor Flux Profiles in the Convective Boundary Layer with Lidar and Radar-RASS. J. Atmos. Oceanic Technol. **11**, 85–93.

Smirnov, M. T., 1984: Modeling the rain microwave thermal emission by Monte Carlo method. Izvestija AS USSR. Physics of the atmosphere and ocean 20, **9**, 721–726.

Shuttleword, W. J., 1988: Macrohydrology – The new challenge for Prosess Hydrology. J. Hydrol. 100, 31–56.

Wilkerson, T. D., G. Schwemmer, B. Gentry and *L. P. Giver*, 1979: Intensities and N_2 collision-broadening coefficients measured for selected H_2O absorption lines between 715 and 732 nm, J. Quant. Spectrosc. Radiat. Transfer **22**, 315–331.